Chapter IV: A Comparison of the Dopamine Binding Sites of the Human Dopamine Receptors

Chapter IV: A Comparison of the Dopamine Binding Sites of the Human Dopamine Receptors

Abstract:

The dopamine neurotransmitter and its receptors play a critical role in such diseases as Parkinson's and schizophrenia. A problem with developing drugs for such diseases is that there are five subtypes of dopamine receptors, only one of which should be affected for each disease. Since the binding sites are quite similar, it is difficult to design the subtype specific agonists and antagonists required for therapy with minimal side effects. This task has been particularly difficult since there are no crystal structures for any dopamine receptors or any closely related G-protein coupled receptors (GPCR) because of the difficulties in crystallizing these membrane-bound proteins.

We have previously reported the 3-D structure of the human D_2 dopamine receptor (hD_2DR), predicted from the primary sequence using *ab initio* theoretical and computational techniques.[1] This 3-D structure was validated by predicting the binding site and relative binding affinities of dopamine plus 3 known dopamine receptor agonists (antiparkinsonian) and 8 known antagonists (antipsychotic) in the hD_2DR receptor. Herein we report the homology structures for the other 4 subtypes of the human dopamine receptors based on the predicted structure of the hD_2DR, and utilize these homology structures to study the dopamine binding site to all 5 receptors. Our studies provide a quantitative, residue-by-residue, contribution of all 5 Å residues to dopamine

and agonist binding, and provide insight into the receptors' ability to differentiate between D_1 and D_2 specific ligands. The predicted structure and the homology structures of the remaining members provide insight into the modifications in the dopamine receptors that allow for differential binding of some ligands but non-discriminatory binding of others, and can be utilized in the design of receptor and subtype specific agonist therapies for maladies such as Parkinson's.

Introduction:

Biogenic amines (such as epinephrine, dopamine, norepinephrine, tryptophan, and serotonin) play an essential role in the central and peripheral nervous systems. These molecules exert their effects by binding to the extracellular surface of a GPCR, which causes changes that lead to activation of a G-protein on the intracellular surface, which in turn leads to a cascade of events in the cytoplasm. GPCRs consist of an extracellular amino terminus, an intracellular carboxy terminal region, and seven □-helical transmembrane (TM) domains. Three intracellular (IC) and three extracellular (EC) loops connect the seven transmembrane domains of the protein.

Dopamine, a catecholamine intermediate in the biosynthesis of epinephrine and norepinephrine, is a particularly well-studied biogenic amine, whose receptors are important targets for treating schizophrenia (antagonists to D_3)[2] and Parkinson's diseases (agonists to D_2)[3]. There are five known human Dopamine Receptors (DRs) with multiple isoforms for each.[4] These DRs are classified on the basis of their pharmacological characteristics into two subfamilies:

- D_1like: D_1 and D_5 show 82% sequence homology. These receptors have a short third intracellular loop (IC3) and a long carboxy terminus.
- D_2like: D_2, D_3, D_4 show 54 to 76% sequence homology (76% homology between D_2 and D_3 and 54% between D_2 and D_4). These receptors have a long IC3 loop and a short carboxy terminus.
- On the other hand the D_1 and D_2 DRs have a sequence homology of only 44%.

Mutational studies have indicated that the IC3 loop is directly involved in G-protein coupling[5], but it is unlikely that these length differences between D_1 and D_2 affect the interaction the binding of dopamine.

Since all five DR's are activated by the same endogenous ligand, dopamine, the binding sites of these receptors are expected to be quite similar. The similarity of elements in the binding site of the dopamine receptors creates a challenge to design agonists and antagonists specific to only one subtype of the DR's, with little or no cross reactivity with other subtypes and other GPCRs with high homology. This difficulty is exacerbated greatly by the lack of an experimental 3-D structure for any DR of any species. Indeed considering GPCRs from all forms of life, there is a single 3-D structure for bovine rhodopsin[6]. The experimental shortcomings are the result of the low expression levels of GPCRs and the difficulties associated with crystallizing a membrane bound protein. Some research groups have attempted to alleviate the problem by building homology models for the D_2DR based on the structure of bacteriorhodopsin[7], or bovine

rhodopsin[8]. Unfortunately, due to the low sequence similarity of 19% between the D_2DR and bovine rhodopsin, these homology models are not accurate enough to be used in design of subtype specific drugs. It must be noted, however, that homology models based on bovine rhodopsin have been invaluable tools in rationalizing the results of biochemical experiments; and, once refined using experimental data and distance restraints, these models could serve as coarse model for design of receptor specific drugs. The true shortcomings of the homology models arise in cases where little or no experimental data is available for refinement of the homology model.

Because sufficiently accurate experimental structures are not available, we have developed computational first principles methods to predict the three-dimensional structures of GPCRs (MembStruk) and to predict the binding site and energy for various ligands to these structures (HierDock). These methods have been validated on bovine rhodopsin[9], human β2-adrenergic receptor [10], and 10 mouse olfactory receptors [11]. Recently we provided and overview of the binding site of agonists and antagonists in the human dopamine D_2DR denoted as hD_2DR[1] predicted using these methods. In this paper, we utilize the previously reported structure of the hD_2DR as a template for homology modeling the other 4 subtypes of the human dopamine receptors to study the binding site of dopamine; from these comparative studies, we have gained great insight into the changes in the receptor that bring about the differential binding of ligands to each receptor. The residues involved in recognizing dopamine and their contributions to the binding energy are also described herein. The results from *ab initio* and homology model structures are in excellent agreement with the experimental data on the binding sites and

ligand affinities to the hD_xDR (where x=1, 2, 3, 4 or 5), validating these structures. In addition, we have gained new insights about the characteristics of these receptors and the modifications resulting in differential binding of ligands. Our results are likely to stimulate experiments and are useful for design of subtype specific ligands for dopamine receptors. The validation of the computational techniques for these well-characterized systems, allows for the use of these methods to be extended to other GPCR targets where little experimental information is known.

Materials and Methods:

Choice of forcefields (FF): All calculations for the protein used the DREIDING FF[12] with charges from CHARMM22[13] unless specified otherwise. The non-bond interactions were calculated using Cell Multipole Method[14] in MPSim[15]. The ligands were described with the DREIDING FF using Gasteiger charges[16]. For the lipids we used the DREIDING FF with QEq charges[17]. Some calculations were done in the vacuum (e.g., final optimization of receptor structure to approximate the low dielectric membrane environment). Most calculations treated the solvent (water) using the Analytical Volume Generalized Born (AVGB) approximation to Poisson-Boltzmann solvation model[18].

MembStruk Structure Prediction Method: The MembStruk procedure version MembStruk3.0 used to predict the three dimensional structure of hD_2DR is described in detail in *reference 9*. Here we detail the steps that are relevant to the prediction of hD_2DR. The various steps of the MembStruk procedure are as follows:

The seven TM boundaries of the hD_2DR were predicted using TM2ndS[9b] procedure. Twenty sequences of D_2DR across many species were aligned using multiple sequence alignment program CLUSTALW[19].

This alignment was used to predict the TM regions using TM2ndS. The predicted TM regions of the human D_2 dopamine receptor are shown in **Scheme 4-1**. It is seen that the seven TM helices in hD_2DR are of different length and also are different in length from the corresponding TM helices of rhodopsin. We built 7 canonical α-helices, and then constructed the TM seven helical barrel with the helical axes positioned based on the 7.5 Å three-dimensional density map of frog rhodopsin[20].

(a) We then performed optimization of the translational orientation of the canonical helices by using the hydrophobic center algorithm described in *reference 9*. The maximum hydrophobic centers of the seven helices are residue 17 for TM1, residue 13 for TM2, residue 11 for TM3, residue 11 for TM4, residue 13 for TM5, residue 15 for TM6 and residue 16 for TM7. These hydrophobic centers were fitted to a plane and thus an optimum of relative translational orientation of the helices was obtained.

(b) The rotational orientation of the canonical helices was also optimized using the multisequence hydrophobicity moments, of the middle third of each helix about their maximum hydrophobic center and were optimized based on energy. These

analyses yielded a clear consensus on which residues should contact the membrane and which should face the receptor interior.

(c) The canonical helices were optimized with NEIMO torsional dynamics[21] or Cartesian dynamics (described with the DREIDING FF and Charmm22 charges), for 500 ps at 300 K constant temperature and picked the minimum energy conformation from the dynamics. This step optimizes the kinks and bends in the helices.

(d) The helical bundle now has helices with bends and kinks. The rotational orientation of these non-canonical helices was further optimized using both the procedure in step c) followed by energy based optimization called "Rotmin" described in *reference 9*. Steps c), d) and f) is a part of systematic search algorithm for optimum translational and rotational orientation and these steps aid in getting over large barriers for structure optimization.

(e) The optimized TM barrel structure was then equilibrated by immersing it in a bilayer barrel of dilauroylphosphatidyl choline and the full system was optimized with rigid body quaternion molecular dynamics (MD), treating each molecule as a rigid body for 50 ps at constant temperature of 300 K using MPSim code.

(f) The interhelical loops were built using WHAT IF[22] and disulfide bonds were formed between Cys 107 in TM3 and Cys 182 in extracellular loop 2. This full system was then optimized with conjugate gradient minimization technique to 0.1kcal/mol/Å RMS in force.

Homology Structure Prediction Method: We utilized standard homology modeling techniques as described in *references 7-8* to build the 3-D models for the D_1, D_3, D_4 and D_5 subtypes of the human dopamine receptors using the predicted structure of the hD_2DR as the template.

Prediction of Ligand Binding Sites and Binding Energies:

Ligand Structure Preparation: Dopamine shown in **Figure 4-1** was built with chemdraw and the two dimensional structure was converted to three dimensional structures in cerius2. Hydrogens were added with Gasteiger charges assigned also using the concord software. We then minimized the potential energy of each ligand using conjugate gradients to a RMSD in force of 0.1kcal/mol/Å.

Function Prediction: HierDock protocol is a hierarchical strategy of ranging from coarse-grain docking to fine-grain optimization for docking ligands in proteins. This method has been tested for various GPCRs[9-11], membrane proteins[23] and globular proteins[24]. This protocol has been described in detail in these references. In here we use

the version of HierDock2.0 described in *reference 9a*. In brief the various steps of HierDock protocol version 2.0 is as follows:

The HierDock ligand screening protocol follows a hierarchical strategy for examining ligand binding conformations, and calculating their binding energies. The steps are as follows:

1) First we carry out a coarse grain docking procedure to generate a set of conformations for ligand binding in the receptor. Here we use Dock 4.0[25] to generate and score 1000 configurations, of which 10% (100) were selected using a buried surface area cutoff of 90% and using energy scoring from Dock4.0, for further analysis. The options used in Dock4.0 are flexible ligand docking with torsion drive and allowing four bumps.

2) The 100 best conformations selected for each ligand from step a) are subjected to all-atom minimization keeping the protein fixed but the ligand movable. The solvation of each of these 100 minimized structures was calculated using the Analytical Volume Generalized Born (AVGB) continuum solvation method[18]. Then the 10 best structures based on the potential energy of the ligand in the protein, were selected from these 100 structures for the next step.

3) Next we optimize the structure of the receptor/ligand complex allowing the structure of the protein to accommodate the ligand. This is essential to identify the optimum conformations for the complex. The all-atom receptor/ligand energy minimization was performed on the 10 structures from the previous step. Using these optimized structures, we calculate the binding energy (BE) using the equation:

$$BE = PE \text{ (ligand in protein)} - PE \text{ (ligand in solvent)} \quad (1)$$

as the difference between the energy of the ligand in the protein and the energy of the ligand in water. The energy of the ligand in water is calculated using DREIDING FF and the SGB or AVGB continuum solvation method[18].

4) Next we select from the five structures from step 3, the one with the maximum number of hydrogen bonds between ligand and protein. For this structure we use the SCREAM side chain replacement program to reassign all side chains for the residues within 5 Å in the binding pocket [this uses a side-chain rotamer library (1478 rotamers with 1.0Å resolution) with the all-atom DREIDING energy function to evaluate the energy for the ligand-protein complex. The binding energy of all the 5 optimized complexes is calculated.

Locating the Putative Binding Site: To locate the binding site of dopamine, other agonists and antagonists, we scanned the entire D_2DR structure without any knowledge of

the binding site. The molecular surface of the entire receptor structure was mapped using autoMS utility of DOCK4.0[25]. Spheres were generated to fill up the void regions of the entire receptor using sphgen utility of Dock4.0. The program "Pass"[26] was then used to locate plausible centers of large void regions in the receptor. The spheres that are within 5.0 Å of these centers are gathered for docking of ligands. For D_2DR we obtained 9 regions where we applied the ScanBindSite protocol for each region, with the following docking steps:

ScanBindSite: Figure 4-2 shows the results of the "ScanBindSite" procedure for D_2DR for dopamine. A tolerance of 30kcal/mol is used since the minimization of the ligand with the fixed receptor structure is done for a fixed number of 50 steps.

Prediction of binding sites and binding energies: We used HierDock protocol steps a) to d) to dock dopamine to region 1. HierDock protocol steps a) to d) were applied to these regions and the best 5 bound structures for each ligand was chosen.

Refinement of the bound structures: The binding site of the best-bound structures for each ligand was further refined using the following procedure. The docked structures were fully minimized for 5000 steps or 0.1 RMS deviations. Residues in the 5.5 Å vicinity of the ligand were replaced with alanine. Conjugate gradient minimization was carried out for 5000 steps or 0.1 kcal/mol/Å RMS deviations to relax the ligand in the active site. This would allow the ligand to optimize in the putative binding cavity. The

side chain rotamers of the residues were replaced using SCREAM side chain placement program and the ligand/receptor complex was again minimized in energy for 5000 conjugate gradient steps or 0.1kcal/mol/Å RMS deviations. The binding energies were calculated suing equation (1).

The final docked conformation of dopamine in the hD_2DR receptor was transferred to the other 4 proteins by aligning the protein backbone and transferring the ligand to the new target. Conjugate gradient minimization was carried out for 5000 steps or 0.1 kcal/mol/Å RMS deviations to relax the ligand in the active site. This would allow the ligand to optimize in the putative binding cavity. The side chain rotamers of the residues were replaced using SCREAM side chain placement program and the ligand/receptor complex was again minimized in energy for 5000 conjugate gradient steps or 0.1kcal/mol/Å RMS deviations. The binding energies were calculated suing equation (1).

The Ballesteros & Weinstein General Indexing Method for Residue Numbering: In order to simplify the comparison of aligned residues in different GPCRs, we will utilize the numbering method of Ballesteros and Weinstein (B&W)[27]. The B&W nomenclature assigns the most conserved residue in each transmembrane segment with an index number of 50. For example, Asn is the most conserved residue in TM1 (this is Asn55 in rhodopsin) and this residue is designated as $Asn^{1.50}$ where 1 stands for the transmembrane helix that the residue belongs to. Based on this nomenclature, the residue immediately before Asn in TM1 is denoted as 1.49 and the residue immediately after is denoted 1.51 et cetera. This method facilitates comparison among different GPCRs by using the most

conserved residue in each helix as a reference point. The index residue in each transmembrane segment of rhodopsin is Asn55$^{1.50}$, Asp83$^{2.50}$, Arg135$^{3.50}$, Trp161$^{4.50}$, Pro215$^{5.50}$, Pro267$^{6.50}$, and Pro303$^{7.50}$. All of these residues are 99%-100% conserved in the dopamine systems amongst all organisms and therefore allow unambiguous alignment of the transmembrane of these receptors.

Results:

Dopamine Binding Site to D_1: The dopamine is bound between the water accessible void of TM3, 4, 5 and 6 (**Figure 4-3**). The amino group is salt bridged to Asp103 (residue 3.32 of the B&W nomenclature) with a bidentate interaction of 2.7 Å *(-50.970 kcal/mol contribution to binding energy: VDW (-0.497); Coulomb (-39.285*); *Hbond (-11.188).* An additional contact, although unfavorable, is provided to the amino group by Trp99 (3.28) which also makes a 2.8 Å interaction *(1.383 kcal/mol contribution to binding energy: VDW (-0.133); Coulomb (1.864); Hbond (-0.338)).* This interaction is deemed unfavorable since the partially positive hydrogen of the indole ring is pointed towards the protonated amino group of dopamine. In general, it appears that for receptors where the 3.28 residue is a tryptophan, the interaction of the conserved TM3 aspartate 3.32 is reduced with the protonated amino group of dopamine since the interaction is shared with the tryptophan 3.28. Asn292 (6.55) provides an additional contact to the amino group of dopamine *(3.722 kcal/mol contribution to the binding energy: VDW (-0.032); Coulomb (3.754); Hbond (0.000)).* This residue is ~ 4.5 Å away from the protonated amino group yet may be used in the design of favorable antagonists and or agonists. The catechol portion of dopamine is hydrogen bonded to a network of TM5 serines. There is a 3.2-Å hydrogen bond between Ser198 (5) (5.42)

(1.079 kcal/mol total contribution to the binding energy: VDW (-0.168); Coulomb (1.247); Hbond (0.000)) and the *meta*-hydroxyl of dopamine, and a 3.1 Å interaction between Ser202 (5) (5.46) *(-2.122 kcal/mol total contribution to the binding energy: VDW (-0.134); Coulomb (0.111); Hbond (-2.189))* and the *para*-hydroxyl of dopamine. Ser199 (5.43) is within 4.3 Å but is too far to form contacts that could be considered hydrogen bonds, although it does contribute favorably to the binding energy via a Coulombic interaction *(-2.319 kcal/mol total contribution to the binding energy: VDW (-0.041); Coulomb (-2.277); Hbond (0.000))*. Regardless, however, all three serines may contribute positively to the binding of dopamine to this receptor if we assume that rotation leading to activation may occur. A fourth serine in TM3 (Ser107 (3.36)) also appears to have minimal favorable interaction with the aromatic portion via a sigma-pi interaction between the hydroxyl hydrogen and the aromatic system *(-0.435 kcal/mol total contribution to binding energy: VDW (-0.104); Coulomb (-0.331); Hbond (0.000).* Ser107 (3.36) is most suited for hydrogen bonding with heteroatom of ligands such as 6-hydroxy dopamine.

There are several aliphatic contacts such as Ala195 (5.39), which is significant in contributing to the binding energy *(-6.000 kcal/mol contribution to the binding energy: VDW (-0.006); Coulomb (-5.994); Hbond (0.000),* and the first aromatic micro-domain, which in this case is very significant in ligand binding. Trp285 (6.48) *(-1.322 kcal/mol total contribution to binding energy: VDW (-0.310); Coulomb (-1.012); Hbond (0.000))*, Phe289 (6.52) *(-0.508 kcal/mol total contribution to the binding energy: VDW (-0.508); Coulomb (0.000); Hbond (0.000)*, and Phe156 (4.54) *(-0.012 kcal/mol total contribution to the binding energy: VDW (-0.012); Coulomb (0.000); Hbond (0.000))*, comprise the aromatic micro-domain present in TM4 and TM6 which stabilize the aliphatic/aromatic portions of the dopamine ligand. Val152 (4.50), which is

substituted, with a tryptophan in the D_2-like family of dopamine receptors is the second residue in TM4, which makes up the first aromatic micro-domain. Mutation of this residue to a valine has removed this residues contribution to the binding energy; this residue is no longer in immediate contact with the ligand. A significant additional aliphatic contact is provided by Tyr194 (5.38), *(-9.034 kcal/mol total contribution to the binding energy: VDW (-0.025); Coulomb (-9.009); Hbond (0.000)).* Trp148 (4.46) is located two turns of the helix below Phe156 (4.54) *((0.000 kcal/mol total contribution to the total binding energy: VDW (0.000); Coulomb (0.000); Hbond (0.000))* and is within 7 Å of the ligand and could be used as a favorable contact point in designing D_1 specific ligands. Val100 (3.29), Ile111 (3.40), Ile201 (5.45), Phe288 (6.51), and Val317 (7.39) are also within the dopamine-binding pocket; however, they do not contribute at all to the binding of dopamine. It must be noted, however, that these residues must be taken into account in designing receptor specific ligands.

Dopamine Binding Site to D_2: We find the following residues (**Figure 4-4**) to be essential for binding of dopamine in the human D_2 receptor: 1) Asp114 (3.32) *(-61.817 kcal/mol total contribution to the binding energy: VDW (-0.474); Coulomb (-50.364); Hbond (-10.979))*: the carboxyl group of the aspartate forms a tight salt bridge (2.6Å) with the primary amino group of dopamine. This residue is conserved over all five human dopamine receptors, as well as in all human biogenic amine receptors. Mutation studies have implicated this residue in the direct binding of the dopamine to D_2. It is important to note that the aspartate in the D_2 receptor provides ~10 kcal/mol more contribution than the aspartate in the D_1 receptor to dopamine binding. Again, it must be noted that the

presence of the tryptophan at the 3.28 position in the D_1 receptor causes the aspartate to share its electrons with both the tryptophan and the ligand; in D_2 the tryptophan is replaced with a phenylalanine; therefore, there is no need for the aspartate to share its electrons with the aromatic. The main component that differs in binding appears to be in the columbic component. 2) Ser193 (5.42) *(0.071 kcal/mol total contribution to binding energy: VDW (-0.432); Coulomb (0.503); Hbond (0.000))* and Ser197 (5.46) *(3.562 kcal/mol: VDW (-0.199); Coulomb (4.057); Hbond (-0.296))* they hydrogen bond to the *meta*-hydroxyl (2.7Å) and *para*-hydroxyl groups (2.7Å), respectively, of the catechol ring of dopamine, playing an essential role in recognizing dopamine. These two residues are conserved over all five human dopamine receptors; although these residues do not appear to be essential for binding, they are necessary for receptor activation. Ser194 (5.43) *(-1.874 kcal/mol contribution to the total binding energy: VDW (-0.126); Coulomb (-0.306); Hbond (-1.442))*, is too far to form a hydrogen bond, yet contributes to both recognition and binding of dopamine to the receptor. In our structure, Ser194 is hydrogen bonded to the backbone nitrogen of residue 192, rather than dopamine. However, it might serve as an alternate to Ser193 in hydrogen bonding to the *meta*-hydroxyl group of the catechol, for the slightly modified structure of the receptor that might result from activation. 3) Phe110 (3.28) *(-1.566 kcal/mol contribution to the total binding energy: VDW (-0.067); Coulomb (-1.498); Hbond (0.000)),* Met117 (3.35) *(-0.151 kcal/mol total contribution to the total binding energy: VDW (-0.151); Coulomb (-0.113); Hbond (0.000))*, Cys118 (3.36) *(-1.878 kcal/mol contribution to the total binding energy: VDW (-0.160); Coulomb (-1.718); Hbond (0.000)),* Phe164 (4.54) *(0.495 kcal/mol total contribution to the binding energy: VDW (-0.083); Coulomb (0.578); Hbond (0.000)),* Phe189 (5.38) *(-5.752 kcal/mol total contribution to the binding energy: VDW (-0.044); Coulomb (-5.709); Hbond (0.000)),* Val190 (5.39) *(-3.787 kcal/mol*

contribution to the total binding energy: VDW (-0.244); Coulomb (-3.540); Hbond (-0.003)), Trp386 (6.48) *(-1.036 kcal/mol contribution to the total binding energy: VDW (-0.224); Coulomb (-0.813); Hbond (0.000))*, Phe390 (6.52) *(-2.102 kcal/mol contribution to the total binding energy: VDW (-0.640); Coulomb (-1.462); Hbond (0.000))*, and His393 (6.55) *(-9.726 kcal/mol total contribution to the binding energy: VDW (-0.015); Coulomb (-9.711); Hbond (0.000))*, Ile394 (6.56) (which is the sole difference between the D_2 and D_3 dopamine binding pocket and possibly a point of differentiation) form a mostly hydrophobic pocket for the dopamine. Of the conserved WXPFF motif, we find Trp386 (6.48) and Phe390 (6.52) are within the 4.5 Å binding pocket, but Phe389 (6.51) is at 7.2 Å and does not contribute to the binding energy. Other residues present in the cavity but not contributing to the binding energy include: Val111 (3.29), Ile394 (6.56), and Thr412 (7.39).

Two amino acid contacts contribute unfavorably to the binding of dopamine but are not directly present in the cavity. Tyr191 (5.40) *(4.892 kcal/mol total contribution to the binding energy: VDW (-0.005); Coulomb (4.897); Hbond (0.000))* is destabilizing dopamine binding due to the repulsion between the oxygen of dopamine and the oxygen of tyrosine ring. Interestingly, Ile194 (5.43) *(2.870 kcal/mol total contribution to the binding energy: VDW (0.000); Coulomb (2.870); Hbond (0.000))* also contributes unfavorably to dopamine binding due the Van der Waals clash with the ring.

Dopamine Binding Site to D_3: The binding site of dopamine to the human D3 dopamine receptor is shown in **Figure 4-5**. The amino group of dopamine is once again very tightly salt bridged to Asp110 (3.32) *(-60.101 kcal/mol total contribution to the binding energy: VDW (-*

0.529); Coulomb (-48.581); Hbond (-10.991)) in a bidentate fashion with distances of 2.8 Å. His349 (6.55) provides a second interaction with the protonated amino group of dopamine *(-4.096 kcal/mol total contribution to the binding energy: VDW (-0.047); Coulomb (-4.049); Hbond (0.000)),* and a cation/pi interaction with Phe106 (3.28) *(-0.060 kcal/mol total contribution to the binding energy: VDW (-0.060); Coulomb (0.000); Hbond (0.000)).* Additional residues such as Cys114 (3.36) *(-0.246 kcal/mol total contribution to the binding energy: VDW (-0.188); Coulomb (-0.058); Hbond (0.000))*, and Met113 (3.35) *(-0.481 kcal/mol total contribution to the binding energy: VDW (-0.042); Coulomb (-0.439); Hbond (0.000))* interact favorably with dopamine. The catechol of dopamine is hydrogen bonded to the network of TM5 serines: Ser192 (5.42) *(-0.088 kcal/mol total contribution to the binding energy: VDW (-0.481); Coulomb (0.401); Hbond (-0.008))*, Ser193 (5.43) *(4.368 kcal/mol total contribution to the binding energy: VDW (-0.066); Coulomb (4.685); Hbond (-0.252)),* and Ser196 (5.46) *(-0.542 kcal/mol total contribution to the binding energy: VDW (-0.141); Coulomb (-0.397); Hbond (-0.004)).* Ser193 actually has a destabilizing effect on dopamine binding to this receptor. The distances for the interactions of the triplet serines are 2.8, 3.9, 2.9 Å, respectively. Additional aliphatic stabilization is caused by the aromatic micro-domain consisting of Phe162 (4.54) *(-0.083 kcal/mol total contribution to the binding energy: VDW (-0.083); Coulomb (0.000); Hbond (0.000))*, Trp342 (6.48) *(-1.234 kcal/mol total contribution to the binding energy: VDW (-0.216); Coulomb (-1.018); Hbond (0.000)),* Phe346 (6.52) *(-0.536 kcal/mol total contribution to the binding energy: VDW (-0.536); Coulomb (0.000); Hbond (0.000)),* and the aliphatic Phe188 (5.38) *(-5.762 kcal/mol total contribution to the binding energy: VDW (-0.029); Coulomb (-5.733); Hbond (0.000)).* Val189 (5.39) *(1.902 kcal/mol total contribution to the binding energy: VDW (-0.169); Coulomb (2.071); Hbond (0.000))* is slightly energetically destabilizing. Val350 (6.56) is the sole residue that is different between the D_2 and D_3 dopamine binding pockets and is possibly responsible for the differential binding of

dopamine and other ligands although it does not contribute at all to the binding of dopamine. Other residues that are present in the dopamine binding pocket but do not contribute to the binding of the ligand include: Val107 (3.29), Trp158 (4.50), and Phe345 (6.51).

Interestingly, dopamine has both an experimental and a theoretically calculated higher affinity to the D_3 receptor. An analysis of the cavity reveals that Thr369 (7.39) (also present in D_2 (Thr412)) is very favorably contributing to the binding of dopamine. Whereas in the D_2 dopamine binding site, Thr412 contributed less than 0.5 kcal/mol to the binding of dopamine, in the D_3 structure, Thr369 contributes over 13 kcal/mol to the binding *(-13.585 kcal/mol total contribution to the binding energy: VDW (-0.009); Coulomb (-13.576); Hbond (0.000)*. This is a significant energetic contribution. Based on these studies, mutation of this threonine to alanine must significantly reduce dopamine's affinity to this receptor.

Additional studies have also implicated the second extracellular loop (EC2) as being important in discriminating between dopamine, agonists, and antagonists. Our analysis of the EC2 loop has shown several major modifications in the loop that may be responsible for discriminating and differential binding.

A recent study by our group has identified candidate residues to be mutated in order to gain better insight into possible residue contacts causing D_2 and D_3 specificity. We have successfully mapped both agonist and antagonist cavities and identified residues that are different between the two receptors. A brief portion of our data is shown in

Scheme 4-2. The residues in red are those residues that have been altered in the vicinity of the binding pockets. The residues in green are those residues that face the cavity or are significant changes in amino acid nature. We have identified a total of 21 residues for both agonists and antagonists. Of these 21 predictions, 14 are within contact distance of 5-6 Å of the ligand in the agonist/dopamine-binding site.

Residues in red represent those changes, which are not deemed significant, as the nature of the amino acid does not change. Residues in green represent those changes, which are inside the cavity or may possibly change the affinity and preference of the receptor for a ligand, and may thus be useful for receptor specific drug design.

For D_2-D_3 Dopamine/Agonist Specificity Studies Mutate:

S163 and T165 in TM4

A177, Q179, E181, I183, A185, A188 in EC2 and TM5

I391, I394, I397, D400, P404, V406 in TM6 and EC3

Interestingly, it should be noted that the residue modifications in TM1 provide for special opportunities for designing receptor specific antagonists. These modifications have been previously unused in structure-based rational drug design since no structure has been available. Additionally, modifications in the extracellular loops may serve as an excellent opportunity for receptor specific drug design.

Dopamine Binding Site to D_4: The dopamine binding site is shown in **Figure 4-6**. Dopamine is salt bridged via its amino group to Asp115 (3.32) *(-58.608 kcal/mol total contribution to the binding energy: VDW (-0.555); Coulomb (-48.476); Hbond (-9.576))* with a distance of 2.8 Å. The aromatic 3.28 residue in TM3 has been replaced by a Leu111 (3.28) *(-0.022 kcal/mol total contribution to the binding energy: VDW (-0.022); Coulomb (0.000); Hbond (0.000))*. There is no longer a source for cation/pi interaction, and hence the contribution to the binding energy of the residue at this position is decreased. The methionine at the 3.35 position is replaced with a leucine *(-0.009 kcal/mol total contribution to the binding energy: VDW (-0.009); Coulomb (0.000); Hbond (0.000))*. This modification is similar in nature, but a leucine is much smaller than a methionine. Therefore, the cavity is larger and more accessible for fitting larger ligands. Cys119 (3.36) *(-0.053 kcal/mol total contribution to the binding energy: VDW (-0.299); Coulomb (0.245); Hbond (0.000))* provides minor energetic stabilization for dopamine, but may be used to stabilize antagonists as has been shown in the experimental literature. His414 (6.55) *(-10.627 kcal/mol total contribution to the binding energy: VDW (-0.218); Coulomb (-8.380); Hbond (-2.029))* provides a significant favorable energetic contribution towards binding. The catechol hydroxyls are hydrogen bonded to Ser196 (5.42) *(-4.080 kcal/mol total contribution to the binding energy: VDW (-0.222); Coulomb (-3.811); Hbond (-0.047)),* Ser197 (5.43) *(-0.032 kcal/mol total contribution to the binding energy: VDW (-0.072); Coulomb (0.040); Hbond (0.000)),* and Ser200 (5.46) *(-2.836 kcal/mol total contribution to the binding energy: VDW (-0.149); Coulomb (0.078); Hbond (-2.764))* all in TM5. The hydrogen bonding contacts are 3.4 Å to the *meta*- and 3.2 Å to the *para*-hydroxyl. Ser196 is a major contributor to the binding of dopamine to this receptor.

The aliphatic and aromatic portions of dopamine are stabilized by the aromatic micro-domain consisting of Trp407 (6.48) *(-1.355 kcal/mol total contribution to the binding energy: VDW (-0.317); Coulomb (-1.038); Hbond (0.000)),* and Phe411 (6.52) *(-0.536 kcal/mol total contribution to the binding energy: VDW (-0.536); Coulomb (0.000); Hbond (0.000)).* Phe160 (4.50) and Ala164 (4.54) comprise the other half of the aromatic micro-domain, but are not present within 6 Å mainly due to the exchange of phenylalanine to alanine. Ile415 (6.56) *(-0.023 kcal/mol total contribution to the binding energy: VDW (-0.023); Coulomb (0.000); Hbond (0.000)),* and Val193 (5.39) *(-4.086 kcal/mol total contribution to the binding energy: VDW (-0.075); Coulomb (-4.011); Hbond (0.000))* provide other aliphatic contacts to dopamine.

Several residues appear in the active site, yet do not contribute to the binding of dopamine in any way. These residues include Met112 (3.29), Tyr192 (5.38) and Phe410 (6.51). Ile415 (6.56) *(-0.023 kcal/mol total contribution to the binding energy: VDW (-0.023); Coulomb (0.000); Hbond (0.000))* provides minor but insignificant Van der Waals contact to the ring.

Dopamine Binding Site to D_5: The dopamine binding site in the D_5 dopamine receptor is shown in **Figure 4-7**. The amino group of dopamine is salt bridged to Asp120 (3.32) *(-50.630 kcal/mol total contribution to the binding energy: VDW (-0.488); Coulomb (-38.906); Hbond (-11.236)).* Again, this contribution is significantly reduced compared to the D_2-like family of dopamine receptors where the 3.28 residue is either a phenylalanine or a leucine. The presence of the tryptophan causes the aspartate to be shared between the ligand and the protein side chains. Regardless, however, the interaction between Asp120 and dopamine is a bidentate interaction of 2.8 Å. Trp116 (3.28) *(1.373 kcal/mol total contribution to the binding*

energy: VDW (-0.149); Coulomb (1.877); Hbond (-0.355)) is causing a destabilizing interaction with the amino group of dopamine. Ser124 (3.36) *(1.758 kcal/mol total contribution to the binding energy: VDW (-0.074); Coulomb (1.832); Hbond (0.000))* creates a sigma-pi interaction with the ring, however, the angle is not adequate and hence the energetic contribution is actually unfavorable. The catechol is hydrogen bonded to the network of serines: Ser229 (5.42) *(0.626 kcal/mol total contribution to the binding energy: VDW (-0.310); Coulomb (0.936); Hbond (0.00)),* Ser230 (5.43) *(-0.085 kcal/mol total contribution to the binding energy: VDW (-0.060); Coulomb (-0.013); Hbond (-0.011)),* Ser233 (5.46) *(-0.645 kcal/mol total contribution to the binding energy: VDW (-0.165); Coulomb (0.233); Hbond (-0.714))* all in TM5 are in hydrogen bond contact with the catechol. Ser229 and Ser233 are within reasonable hydrogen bond distance of 2.9 Å in both cases. Ser230 is within 4.0 Å. The aliphatic and aromatic portions of the ring are stabilized by Tyr225 (5.38) *(-7.335 kcal/mol total contribution to the binding energy: VDW (-0.073); Coulomb (-7.262); Hbond (0.000))*, Trp309 (6.48) *(-1.287 kcal/mol total contribution to the binding energy: VDW (-0.281); Coulomb (-1.006); Hbond (0.000))*, Phe313 (6.52) *(-0.565 kcal/mol total contribution to the binding energy: VDW (-0.565); Coulomb (0.000); Hbond (0.000))*, and Phe173 (4.58) *(-0.042 kcal/mol total contribution to the binding energy: VDW (-0.042); Coulomb (0.000); Hbond (0.000)).* Ala226 (5.39) *(-5.895 kcal/mol total contribution to the binding energy: VDW (-0.007); Coulomb (-5.888); Hbond (0.000))* is a surprising contributor to the binding of dopamine. Incidentally, Ile169 (4.54) is the only difference in the binding pocket of dopamine between D_1 and D_5 (it does not contribute to the binding of dopamine). It is postulated that this residue and possibly some loop residues are responsible for the differential binding of dopamine and other ligands. Asn316 (6.55) *(-9.374 kcal/mol total contribution to the binding energy: VDW (-0.040); Coulomb (-9.333); Hbond (0.000))* provides a major

stabilizing force by interacting favorably with the protonated amino group of dopamine. Several residues, although present in the dopamine-binding pocket, do not contribute to the binding of dopamine to this receptor. These residues include: Val117 (3.29), Ile128 (3.40), Phe312 (6.51) and Val345 (7.39).

Discussion:

D_1like vs. D_2like Receptors: There are several key modifications that allow for differential binding of dopamine to the D_1like vs. the D_2like subtypes of the human dopamine receptors. Key residues involved in determining these specificities include: 1) the TM3 aromatic/aliphatic 3.28 residue (in the case of the human D_1like receptors this residue is a tryptophan, whereas in the D_2like receptors the residue is a phenylalanine (D_2 and D_3) or a leucine (D_4)); 2) the TM3 polar 3.36 residue (in the case of the D_1like receptors this residue is a serine, whereas in the D_2like receptors the residue is a cysteine which is clearly less polar and less capable of forming strong hydrogen bonds); 3) the TM4 arotmatic/aliphatic contacts provided by the 4.50, 4.54, and 4.58 residues (in the case of the D_1like receptors small aliphatic such as alanines provide stabilizing contacts for the aliphatic portions of the dopamine ring in TM4; at similar positions, in the D_2like receptors, however, phenylalanine and tryptophan residues have been placed. This provides for a more constrained cavity in the D_2like receptors, allowing only smaller ligands to bind tightly. Based on this analysis, polycyclic agonists would have a less favorable fit to the D_2like family of receptors; 4) the TM5 aromatic contact provided by the 5.38 residue (in the case of the D_1like receptors the aromatic contact at position 5.38 is a tyrosine, whereas in the D_2like receptors, this is a phenylalanine. The difference in

hydrogen bonding capabilities can be used to design subtype specific agonists); 5) the TM6 polar contact at position 6.55 (in the case of the D_1like receptors, this is an asparagine residue, whereas in the D_2like receptors this is a histidine residue.

The combination of the above named 5 changes in the transmembrane region, along with changes in the second extracellular loop (that are not discussed here) account for the differential binding of the ligand to these two subfamilies of receptors. Although the transmembrane modifications alone do not depict the complete intricacies of dopamine binding and differentiation, they provide an excellent starting point for the design and synthesis of receptor and subtype specific ligands.

Comparison of Individual Receptors:

D_1 vs. D_5: The D_1 and D_5 residues exhibit few differences in the transmembrane portion of the binding site of dopamine. Incidentally, these receptors are exhibit similar binding affinities for dopamine. The single amino acid modification present in the vicinity of dopamine is Ile169 (4.54) is the only difference in the binding pocket of dopamine between D_1 and D_5 (it does not contribute to the binding of dopamine). It is postulated that this residue, and possibly some residues from the second extracellular loop are responsible for the differential binding of dopamine and other ligands, although this differential binding is minor.

D_2 vs. D_3: Similar to the D_1 vs. D_5 case, there is little difference in the binding cavity of the D_2 vs. D_3 receptors in the transmembrane region. Ile394 (6.56) (which is the sole

difference between the D_2 and D_3 dopamine binding pocket and possibly a point of differentiation) does not contribute significantly to the binding energy. Again, it is postulated that residues in the second extracellular loop may be important in causing the differential binding of some ligands to one receptor versus another. In this paper, we have suggested several mutations in both the second extracellular loop, and TM regions that could improve our understanding of the differential binding of these two receptors for classic pharmaceuticals.

D_2 vs. D_4: Due to the essentially identical dopamine binding sites between the D_2 and D_3 receptors, we will forgo the comparison of the D_3 vs. D_4 binding sites, and will focus on the analysis of the D_2 vs. D_4 dopamine binding sites. There are three major differences in the cavity of dopamine between the D_2/D_3 and the D_4 receptor. 1) The aromatic/aliphatic 3.28 residue is a phenylalanine in the D_2/D_3 receptors, but it has been changed to a leucine in D_4; 2) The 3.35 methionine has been mutated to a valine in D_4; 3) The TM5 aromatic 5.38 tyrosine in D_2 has been mutated to a phenylalanine in D_4. These changes, we believe, contribute to the differential binding of dopamine to these receptors and can be used in design of receptor specific drugs.

Conclusion:

Mutation of key residues in the dopamine binding sites of the D_1-D_5 dopamine receptors allow for differentiation of dopamine and other ligands by the receptors. Although analysis shows minor differences in the nature of amino acids present in the cavity, the

change in type of amino acid provides significant differences in binding. Most importantly, we have identified a quantitative energetic contribution of each residue in the dopamine binding cavity; this analysis can be used in performing mutation experiments, and in design of receptor specific agonists resembling dopamine.

Figures:

MDPLNLSWYDDDLERQNWSRPFNGSDGKADRPHYNYYATLLTLLIAVIVFGNV
LVCMAVSREKALQTTTNYLIVSLAVADLLVATLVMPWVVYLEVVGEWKFSRIH
CDIFVTLDVMMCTASILNLCAISIDRYTAVAMPMLYNTRYSSKRRVTVMISIVWV
LSFTISCPLLFGLNNADQNECIIANPAFVVYSSIVSFYVPFIVTLLVYIKIYIVLRRRR
KRVNTKRSSRAFRAHLRAPLKGNCTHPEDMKLCTVIMKSNGSFPVNRRRVEAAR
RAQELEMEMLSSTSPPERTRYSPIPPSHHQLTLPDPSHHGLHSTPDSPAKPEKNGH
AKDHPKIAKIFEIQTMPNGKTRTSLKTMSRRKLSQQKEKKATQMLAIVLGVFIIC
WLPFFITHILNIHCDCNIPPVLYSAFTWLGYVNSAVNPIIYTTFNIEFRKAFLKILHC

Scheme 4-1. The predicted transmembrane regions of the human D_2 dopamine receptor. Residues in red correspond to the transmembrane helices, while the residues in black represent the N & C termini, and the loops connecting the transmembrane domains.

HYNYYA*T*LL*T*LLI*A*V	D2	TM1
HAYYALSYCALILA	D3	
VG *E*W*K*FSRIHCDI	D2	
TGGVWNFSRICCDV	D3	EC1
RVTVMISIVWVLSFTISCPLLFG	D2	TM4
RVALMITAVWVLAFAVSCPLLFG	D3	
LNNA-DQNECIIANPAFVVYSSIVSFYVPFI	D2	EC2 and TM5
FNTTGDPTVCSISNPDFVIYSSVVSFYLPFG	D3	
ITHILNIHCDCNIPPV	D2	TM6 and EC3
LTHVLNTHCQTCHVSPE	D3	
PVLYSAFTWLGYVNSAVNP	D2	TM7
PELYSATTWLGYVNSALNP	D3	

Scheme 4-2. An analysis of differences in the sequences of human D_2 and D_3 dopamine receptors in the transmembrane domains, and the second extracellular loop.

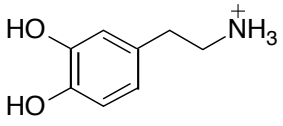

Figure 4-1. The structure of dopamine, a catecholamine neurotransmitter.

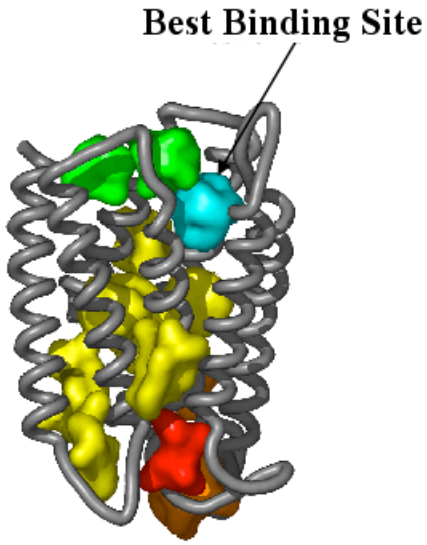

Figure 4-2. The scanning results for D_2DR. Sites are color-coded based on the energy ranges obtained during scanning for ligands in them (-100 – 100=green, 0 - 350=yellow, 200 - 500=orange, 100-900=red). The best identified site for dopamine is colored cyan, and falls into the 'green' energy range. The protein is displayed extracellular side up, with helix I on the far left.

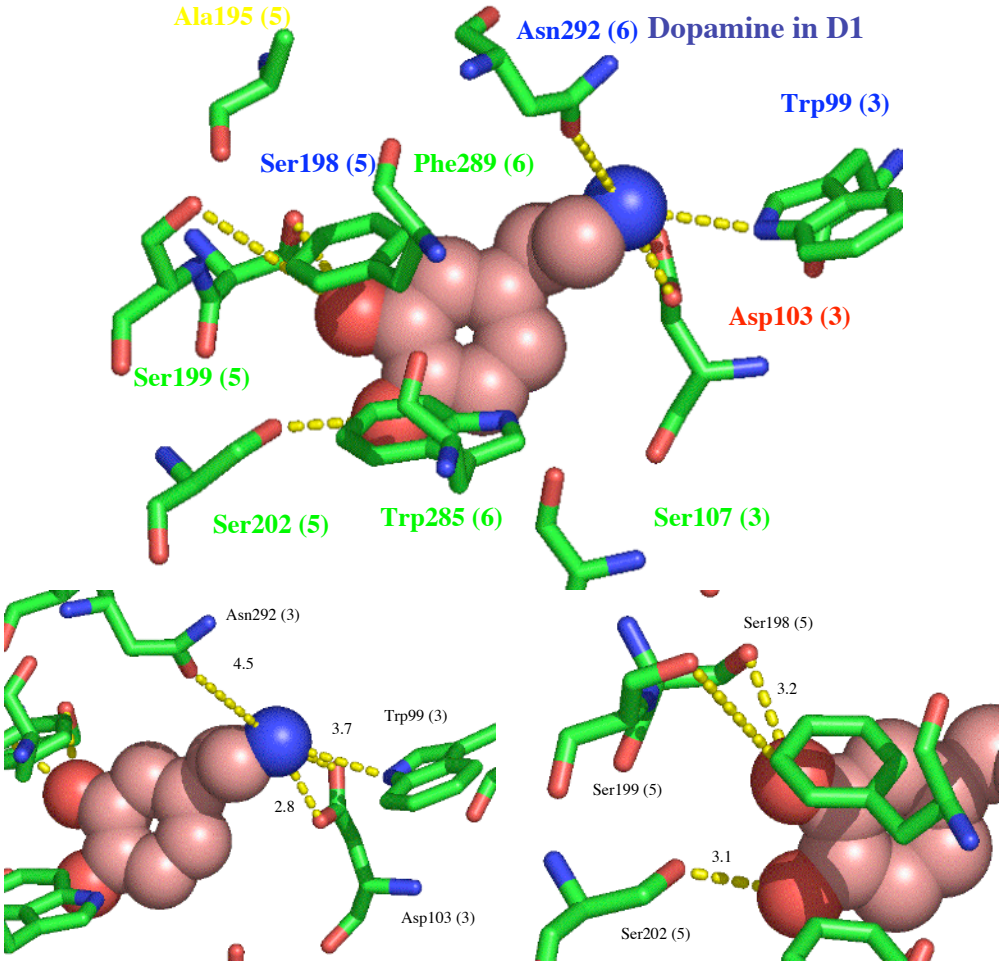

Figure 4-3. The dopamine binding site in the human D_1 dopamine receptor. Details of the salt bridge and hydrogen bonding patterns are shown along with distances.

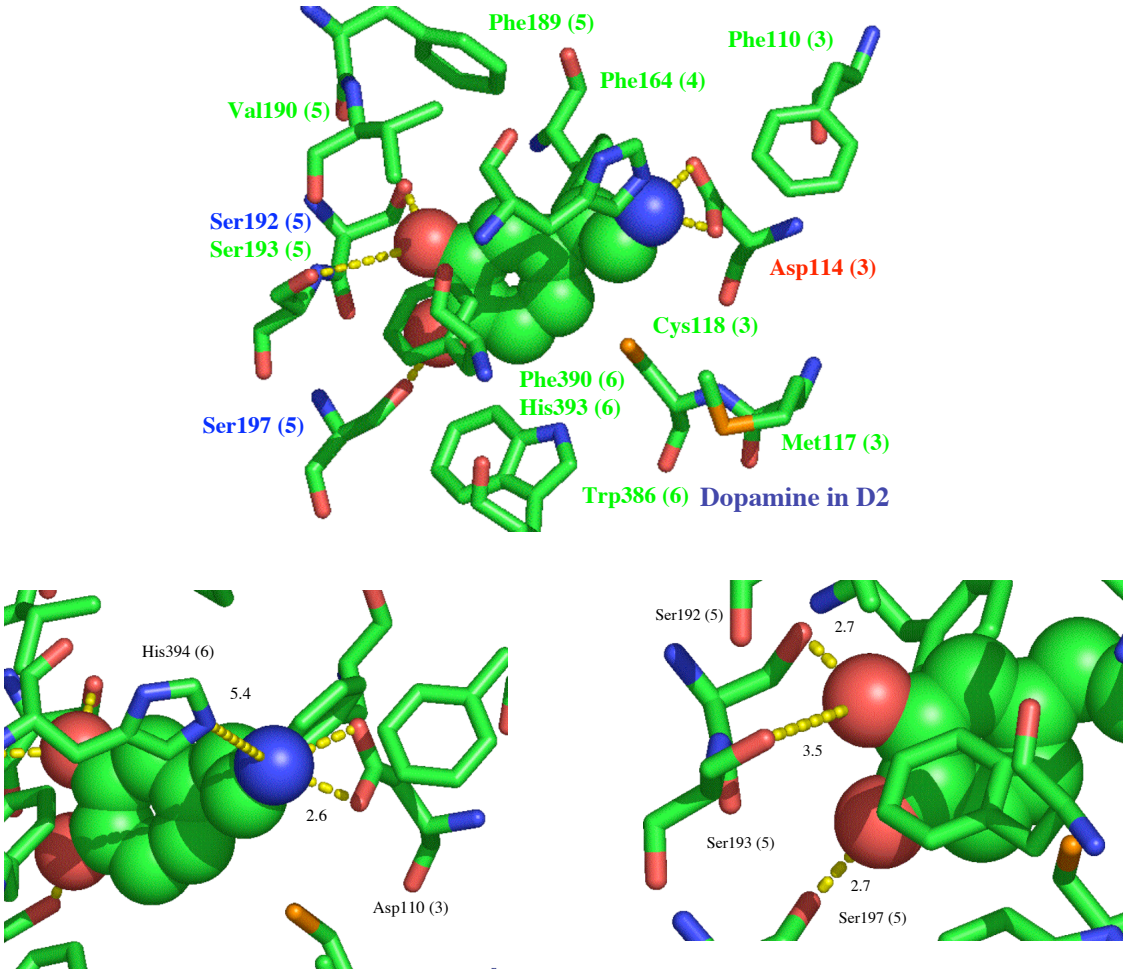

Figure 4-4. The dopamine binding site in the human D_2 dopamine receptor. Details of the salt bridge and hydrogen bonding patterns are shown along with distances.

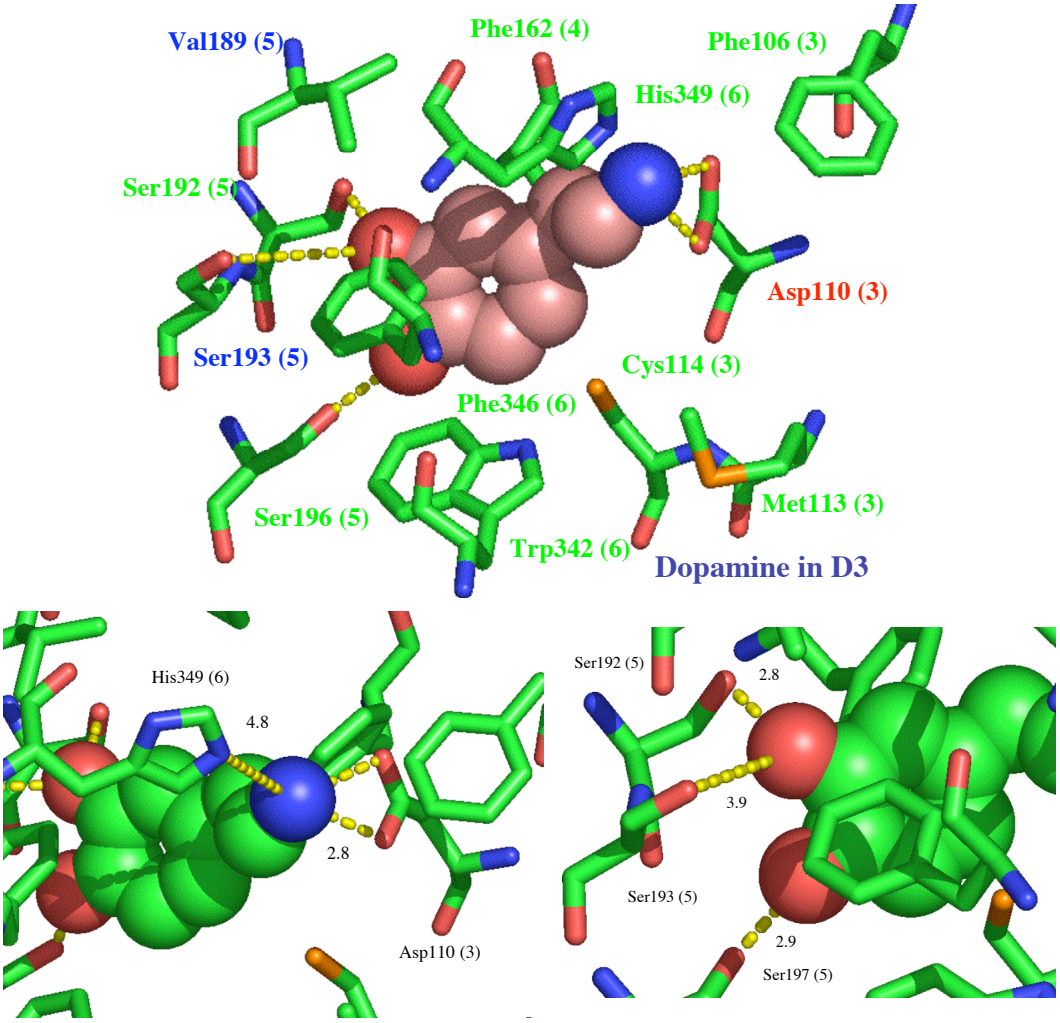

Figure 4-5. The dopamine binding site in the human D_3 dopamine receptor. Details of the salt bridge and hydrogen bonding patterns are shown along with distances.

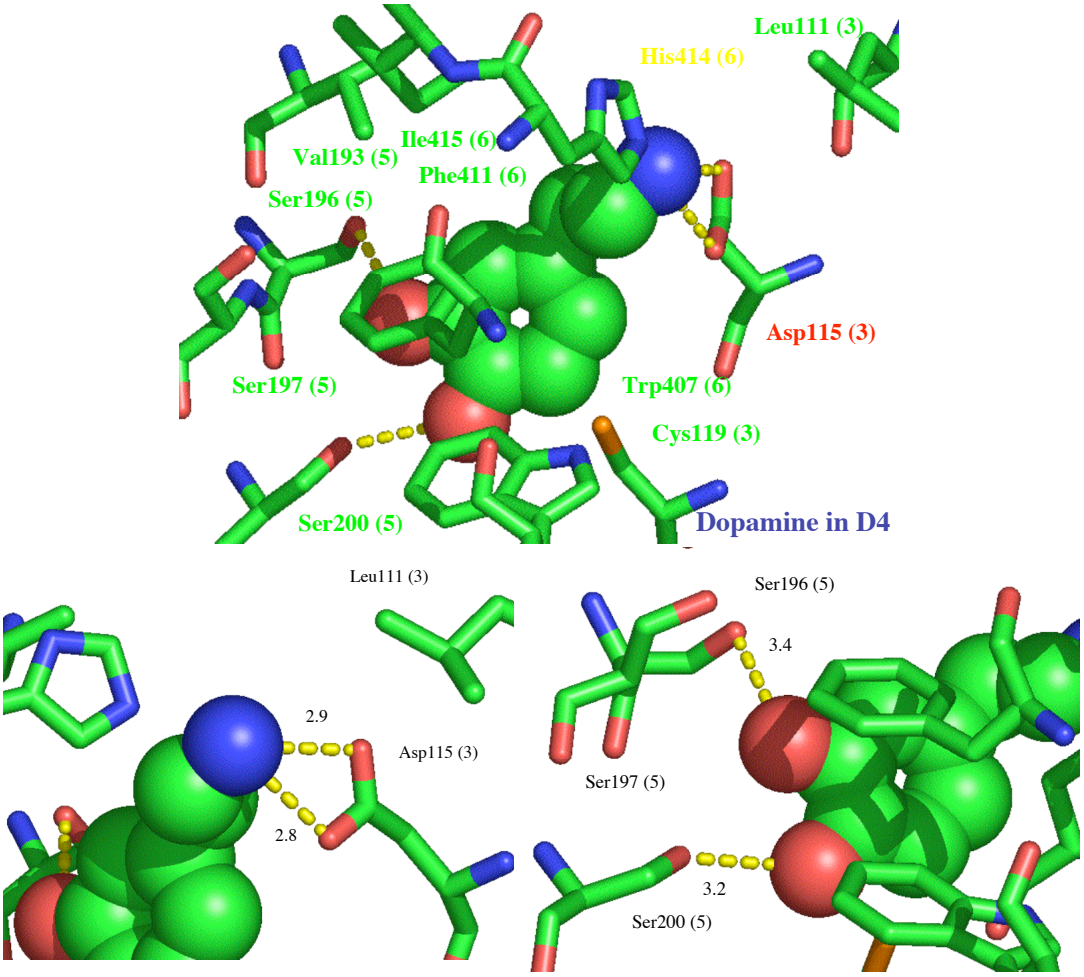

Figure 4-6. The dopamine binding site in the human D_4 dopamine receptor. Details of the salt bridge and hydrogen bonding patterns are shown along with distances.

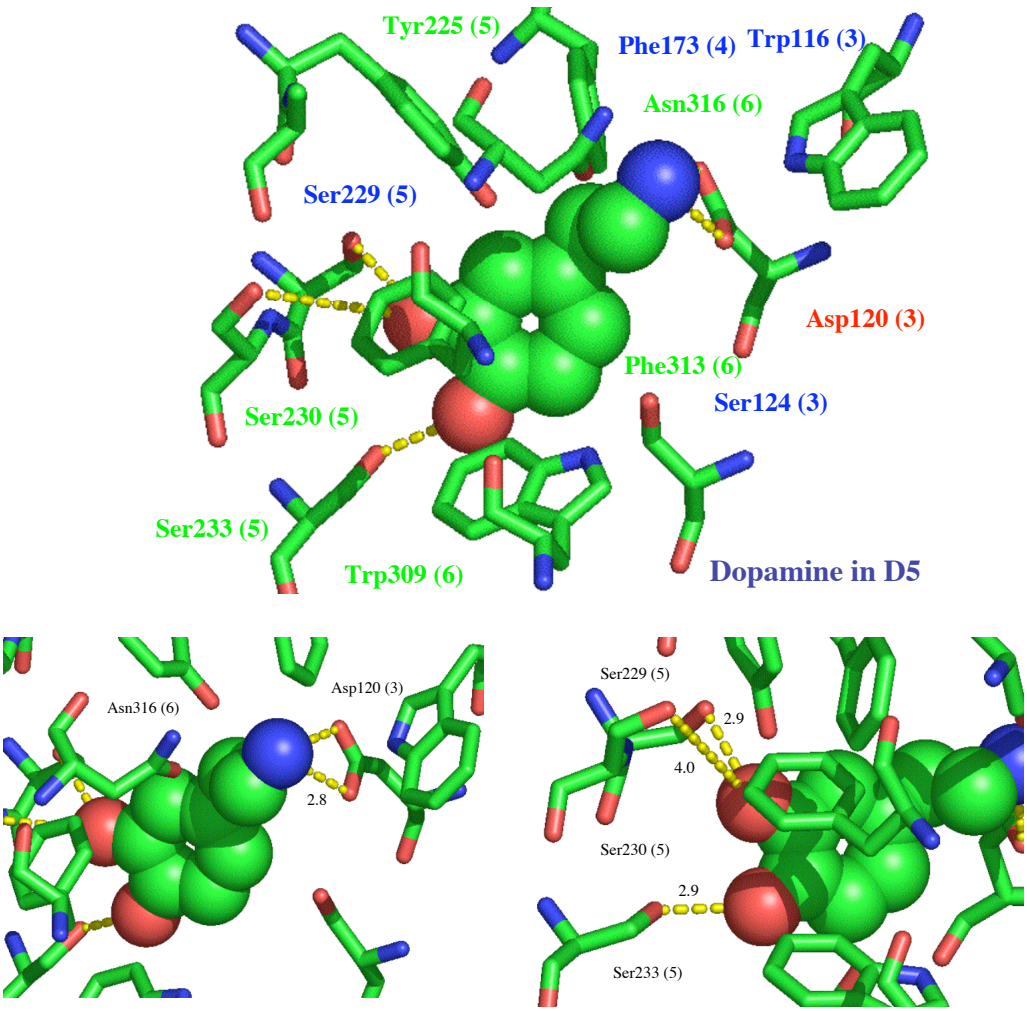

Figure 4-7. The dopamine binding site in the human D_5 dopamine receptor. Details of the salt bridge and hydrogen bonding patterns are shown along with distances.

References:

[1] Kalani M.Y., Vaidehi N., Hall S.E., Trabanino R., Freddolino P., Kalani M.A., Floriano W.B., Kam V., Goddard W.A., III *Proc. Natl. Acad. Sci. USA* 101, 3815-3820 (**2004**).

[2] Jackson D. M., Westlind-Danielsson A. *Pharmacol. Ther.* 64, 291-369 (**1994**).

[3] Strange P.G. *Adv. Drug Res*. 28, 313-351 (**1996**).

[4] Missale C., Nash S. R., Robinson S. W., Jaber M., Caron M.G. *Physiol. Rev.* 78, 189-225 (**1998**).

[5] Kobilka B.K., Kobilka T.S., Daniel K. *Science* 240, 1310 (**1988**).

[6] Palczewski K., Kumasaka T., Hori T., Behnke C. A., Motoshima H., Fox B. A., Le Trong I., Teller D. C., Okada T., Stenkamp R. E. *Science* 289**,** 739–745 (**2000**).

[7] (a) Teeter M.M., Froimowitz M., Stec B., DuRand C.J. *J. Med. Chem* . 37, 2874-2888 (**1994**). (b) Trumpp-Kallmeyer S., Hoflack J., Bruinvels A., Hibert M. *J. Med. Chem.* 35, 3448-3462 (**1992**).

[8] (a) Neve K.A., Cumbay M.G., Thompson K.R., Yang R., Buck D.C., Watts V.J., DuRand C.J., Teeter M.M. *Mol. Pharmacol*. 60, 373-381 (**2001**). (b) Varady J., Wu X., Fang X., Min J., Hu Z., Levant B., Wang S. *J. Med. Chem*. 46, 4377-4392 (**2003**).

[9] (a) Vaidehi N., Floriano W., Trabanino R., Hall S., Freddolino P., Choi E.J., Zamanakos G., Goddard, W.A. *Proc. Natl. Acad. Sci. U.S.A.* 99, 12622-12627 (**2002**). (b) Trabanino R., Hall S.E., Vaidehi N., Floriano W., Goddard, W.A. *Biophys. J.*, in press (**2004**).

[10] Freddolino P., Kalani M.Y., Vaidehi N., Floriano W., Hall S.E., Trabanino R., Kam V.W.T., Goddard, W.A. *Proc. Natl. Acad. Sci. U.S.A.* 101, 2736-2741 (**2004**).

[11] (a) Floriano W. B., Vaidehi N., Goddard W. A., III, Singer M. S., Shepherd G. M. *Proc*. *Natl*. *Acad*. *Sci*. *U.S.A.* 97**,** 10712–10716 (**2000**). (b) Floriano W.B. Vaidehi N., Goddard W.A., III, *Chemical Senses*, in press (**2004**). (c) Hall S.E., Vaidehi N., Floriano W.B., Goddard W.A., III, *Chemical Senses*, in press (**2004**).

[12] Mayo S. L., Olafson B.D., Goddard III, W.A. *J. Phys. Chem.* 94, 8897-8909 (**1990**).

[13] Sali A., Potterton L., Yuan F., van Vlijmen H., Karplus M. *Proteins* 23**,** 318 (**1995**).

[14] Ding H. Q., Karasawa N., Goddard III, W. A. *J. Chem. Phys.* 97, 4309 (**1992**).

[15] Lim K-T, Brunett S., Iotov M., McClurg R.B., Vaidehi N., Dasgupta S., Taylor S., Goddard III, W.A. *J. Comput. Chem.* 18, 501-521 (**1997**).

[16] Gasteiger J., Marsili M. *Tetrahedron* 36, 3219-3228 (**1980**).

[17] Rappé A.K., Goddard III, W.A. *J. Phys. Chem.* 95, 3358-3363 (**1991**).

[18] Zamanakos G., Physics Doctoral Thesis, California Institute of Technology, (**2001**).

[19] Higgins D., Thompson J., Gibson T., Thompson J.D., Higgins D.G., Gibson T.J. *Nucleic Acids Res.* 22, 4673-4680 (**1994**).

[20] Schertler G.F.X. *Eye* 12, 504-510 (**1998**).

[21] (a) Jain A., Vaidehi N., Rodriguez G. *J. Comp. Phys.* 106, 258-268 (**1993**). (b) Vaidehi N., Jain A., Goddard III, W.A. *J. Phys. Chem.* 100, 10508-10517 (**1996**).

[22] Vriend G. *J. Mol. Graph.* 8, 52-56 (**1990**).

[23] Datta D., Vaidehi N., Floriano W. B., Kim K. S., Prasadarao N. V., Goddard W. A., III *Proteins Struct. Funct. Genet.* 50**,** 213–221 (**2003**).

[24] (a) Zhang D., Vaidehi N., Goddard W. A., III, Danzer J. F., Debe D. *Proc. Natl. Acad. Sci. U.S.A.* 99**,** 6579–6584 (**2002**). (b) Wang P., Vaidehi N., Tirrell D. A., Goddard W. A., III *J. Am. Chem. Soc.* 124**,** 14442–14449 (**2002**). (c) Kekenes-Huskey P. M., Vaidehi N., Floriano W. B., Goddard W. A., III *J. Phys. Chem. B* 107**,** 11549–11557 (**2003**). (d) Floriano W. B., Vaidehi N., Zamanakos G., Goddard W. A., III *J. Med. Chem.* 47**,** 56–71 (**2004**).

[25] Ewing T.A., Kuntz I.D. *J. Comput. Chem.* 18, 1175-1189 (**1997**).

[26] Brady P., Stouten F.W. *J. Comp. Molec. Des.* 14, 383-401 (**2000**).

[27] Ballesteros J., Weinstein H. *Methods Neurosci*. 25, 366-428 (**1995**).